Structural and magnetic modulations in $CaCu_xMn_{7-x}O_{12}$

2010 J. Phys.: Condens. Matter 22 186001

(http://iopscience.iop.org/0953-8984/22/18/186001)

J. Phys.: Condens. Matter **22** (2010) 186001 (6pp) doi:10.1088/0953-8984/22/18/186001

Structural and magnetic modulations in $CaCu_xMn_{7-x}O_{12}$

W Sławiński[1], R Przeniosło[1], I Sosnowska[1] and M Bieringer[2]

[1] Institute of Experimental Physics, Faculty of Physics, University of Warsaw, Hoża 69, PL-00 681 Warsaw, Poland
[2] Department of Chemistry, University of Manitoba, Winnipeg, R3T 2N2, Canada

Received 6 January 2010, in final form 14 January 2010
Published 15 April 2010
Online at stacks.iop.org/JPhysCM/22/186001

Abstract
Low temperature atomic position modulations and magnetic moment modulations are reported for $CaCu_xMn_{7-x}O_{12}$ ($x = 0.0$, 0.1 and 0.23) using neutron powder diffraction. Both modulations are described with propagation vectors $(0, 0, q)$ parallel to the c-axis in the hexagonal setting. The present neutron diffraction studies confirm the quantitative model describing the atomic position modulations in $CaCu_xMn_{7-x}O_{12}$ ($x = 0.0$ and 0.1) as derived from synchrotron based powder x-ray diffraction studies (Sławiński *et al* 2009 *Acta Crystallogr.* B **65** 535). Neutron diffraction studies confirm the relation between the atomic position modulation length L_p and the magnetic modulation length $L_m = 2L_p$ between 50 K and the Néel temperature T_N. $CaCu_xMn_{7-x}O_{12}$ ($x = 0.1$ and 0.23) shows a magnetic phase transition near 50 K associated with considerable changes of the magnetic modulation length and the magnetic coherence length, similar to that observed in the parent $CaMn_7O_{12}$.

1. Introduction

Multiferroics are materials which show simultaneous magnetic ordering and electric polarization [1, 2]. The magnetoelectric coupling often leads to changes of the crystal structure and magnetic ordering. Recently the correlation between modulated magnetic ordering and magnetoelectric coupling has been predicted theoretically [3, 4] and has since been observed experimentally in oxides such as $TbMnO_3$ [5], $Ba_2Mg_2Fe_{12}O_{22}$ [6], CuO [5] and $CaMn_7O_{12}$ [7, 8].

The present study focuses on the mixed valent manganite oxides $CaCu_xMn_{7-x}O_{12}$. The $CaCu_xMn_{7-x}O_{12}$ series exhibits unusual physical properties [9] such as multiferroicity, as illustrated by the report of the magnetoelectric effect of $CaMn_7O_{12}$ in [8]. The magnetic phase diagram of $CaMn_7O_{12}$ is complex and involves a modulated magnetic structure [7, 10]. Furthermore a colossal dielectric constant has been reported [11, 12] for $CaMn_7O_{12}$.

Our recent synchrotron radiation (SR) diffraction studies have shown a modulation of atomic positions for $CaMn_7O_{12}$ [13] at low temperatures with significant modulation of the Mn–O bond lengths and Mn–O–Mn bond angles in the crystal lattice [13]. The modulation of atomic positions causes a modulation of the magnetic interactions in the crystal and thus contributes to a modulation of the magnetic moments in $CaMn_7O_{12}$, as shown by neutron diffraction [7, 13].

Neutron diffraction is a very sensitive method for the simultaneous investigation of crystal structures and long range magnetic orderings. The system under investigation is particularly suitable for neutron diffraction due to the neutron scattering length contrast of Ca ($b_{coh} = 4.70$ fm), Cu ($b_{coh} = 7.718$ fm), Mn ($b_{coh} = -3.73$ fm) and O ($b_{coh} = 5.083$ fm) [14]. The present paper reports high-resolution neutron diffraction studies of $CaCu_xMn_{7-x}O_{12}$ at low temperatures. The goal of this study is to provide supplementary information regarding atomic position modulation by means of complementary methods to SR diffraction and to report the spin–lattice coupling in $CaCu_xMn_{7-x}O_{12}$.

2. Experimental details

Polycrystalline samples of $CaCu_xMn_{7-x}O_{12}$ ($x = 0.0$, 0.1 and 0.23) were prepared from stoichiometric amounts of $CaCO_3$ (CERAC, 99.995%), CuO (CERAC, 99.999%) and Mn_2O_3 (CERAC, 99.99%) and reacted in air at 950 °C with KCl as a mineralizer. The synthesis details are presented in [15]. Samples were prepared in several batches where the initial synthesis yielded small quantities of approximately 5 g of $CaCu_xMn_{7-x}O_{12}$ ($x = 0.0$, 0.1 and 0.23). These samples will be referred to as CMO_A, CC1MO_A and CC2MO_A, respectively, and they have already been used in our earlier studies [13, 15, 16]. A second synthesis batch yielded a large

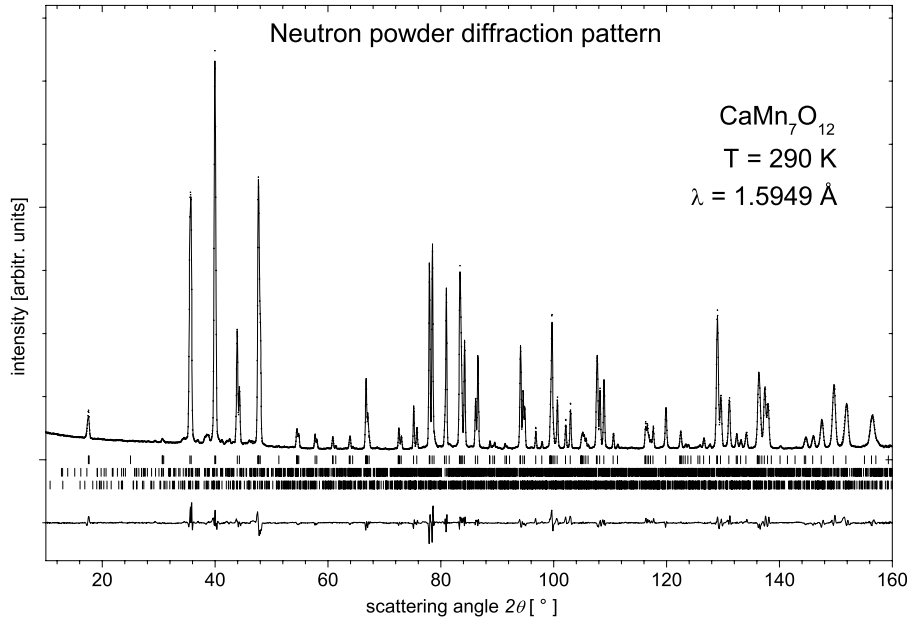

Figure 1. Room temperature Rietveld plot of the neutron powder diffraction pattern ($\lambda = 1.5949$ Å) of $CaMn_7O_{12}$ (sample CMO_B). Solid points = measured data, solid line through the data points = refined profile, solid line at bottom = difference. The three sets of tick marks represent the Bragg positions for $CaMn_7O_{12}$ (top), $CaMn_3O_6$ (middle) and $CaMn_4O_8$ (bottom).

sample of approximately 15 g of undoped $CaMn_7O_{12}$. This new sample will be referred to as CMO_B.

Two sets of neutron powder diffraction experiments were carried out at the Institute Laue Langevin (ILL) in Grenoble. The first set of neutron diffraction experiments was carried out on the high-resolution diffractometer D2B. $CaMn_7O_{12}$ (new sample CMO_B) and $CaCu_{0.1}Mn_{6.9}O_{12}$ (sample CC1MO_A) were placed in cylindrical vanadium containers of 15 mm and 8 mm diameter, respectively. Using a wavelength of 1.595 Å and a scattering vector range $0.35\ \text{Å}^{-1} \leqslant Q \leqslant 7.75\ \text{Å}^{-1}$ (where $Q = \frac{4\pi}{\lambda}\sin\theta$) diffractograms were collected at 10, 60, 100 and 290 K. The diffraction data below 290 K were measured in a Displex. The second set of neutron diffraction measurements were performed with $CaCu_xMn_{7-x}O_{12}$, where $x = 0.0$, 0.1 and 0.23 (CMO_A, CC1MO_A and CC2MO_A) with the high-flux diffractometer D20. The $CaCu_xMn_{7-x}O_{12}$ powder samples were measured in a standard orange cryostat in a cylindrical vanadium container (8 mm diameter). Powder diffraction patterns were recorded from 10 up to 290 K using a neutron wavelength of 2.421 Å covering the scattering vector, Q, range $0.4\ \text{Å}^{-1} \leqslant Q \leqslant 4.9\ \text{Å}^{-1}$. The diffractograms collected on D20 permitted us to follow the temperature dependent magnetic ordering of $CaCu_xMn_{7-x}O_{12}$ ($x = 0.0$, 0.1 and 0.23) with sufficient temperature resolution.

The crystal structure of the new sample CMO_B has also been characterized at RT by using the high-resolution synchrotron radiation powder diffractometer ID31 at the ESRF in Grenoble (France). Small amounts of two impurity phases were found: 2.77(5) vol% of $CaMn_3O_6$ [17] and 4.93(7) vol% of $CaMn_4O_8$ [18] in the in CMO_B sample.

All neutron and SR powder diffraction patterns were analyzed by the Rietveld method [19] using the Jana2006 computer program [20]. The space group $R\bar{3}$ (in hexagonal setting) was used for all the $CaCu_xMn_{7-x}O_{12}$ samples. All atomic positions and separate Debye–Waller factors for each kind of atom were refined.

3. Results

3.1. Modulation of atomic positions

Following previous reports [13, 15, 16, 21, 22] the average crystal structure of $CaCu_xMn_{7-x}O_{12}$ ($x = 0.0$, 0.1 and 0.23), i.e. without modulation of the atomic positions, at low temperature is determined in the hexagonal setting of space group $R\bar{3}$. The initial crystallographic model for the refinement was taken from [13].

Figure 1 shows the Rietveld plot of the refined neutron powder diffraction data for $CaMn_7O_{12}$ (new sample CMO_B) at 290 K. The large scattering Q range and the excellent resolution permitted a more precise determination of the oxide positions than reported in our previous study [13]. Table 1 shows basic crystallographic parameters and agreement factors obtained from $CaMn_7O_{12}$ patterns at 100 and 290 K.

Atomic position modulations were observed in $CaMn_7O_{12}$ and $CaCu_{0.1}Mn_{6.9}O_{12}$ by synchrotron powder x-ray diffraction at temperatures below 250 K and 200 K, respectively [13]. This modulation was described with the superspace group $R\bar{3}(00\gamma)$ and the propagation vector $\vec{q}_p$ parallel to the c axis [13].

Figure 2 shows the temperature dependent powder neutron diffractograms for $CaMn_7O_{12}$ (sample CMO_B) for large diffraction angles; only nuclear peaks are observed because the magnetic form factor value suppresses magnetic peaks at large diffraction angles. The two data sets at 100 and 290 K are above $T_N \approx 90$ K and the remaining two data sets measured at 10 and 60 K are below $T_N \approx 90$ K. Below 290 K satellite Bragg peaks due to atomic position modulation are observed

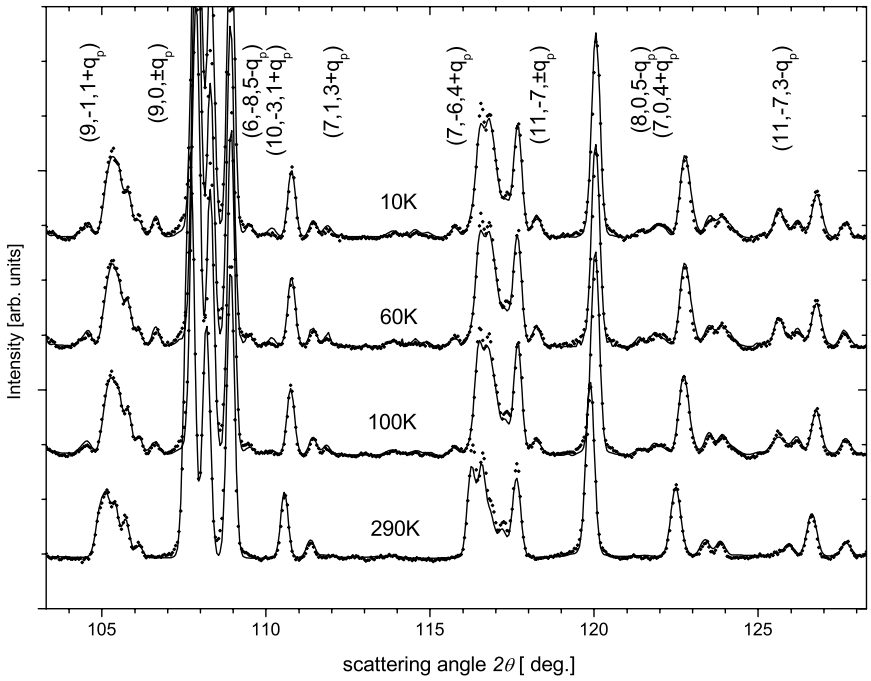

Figure 2. High-angle powder neutron diffractograms (D2B, $\lambda = 1.595$ Å) of $CaMn_7O_{12}$ (sample CMO_B) measured at 10, 60, 100 and 290 K. Solid points = measured data, solid line = calculated profile. The indexing of the satellite maxima is shown.

Table 1. Summary of crystal and experimental data for $CaMn_7O_{12}$ at 100 and 290 K obtained from neutron powder diffraction measurement on D2B (ILL, Grenoble).

Chemical formula	$CaMn_7O_{12}$	$CaMn_7O_{12}$
Space group (average structure)	$R\bar{3}$ (No. 148)	$R\bar{3}$ (No. 148)
Superspace group	$R\bar{3}(00\gamma)0$ (No. 148.1)	—
Temperature (K)	100.0	290.0
$a = b$ (Å)	10.444 44(7)	10.461 27(9)
c (Å)	6.342 71(6)	6.345 20(6)
Volume (Å^3)	599.2051(74)	601.3734(98)
λ (Å)	1.5949	1.5949
Modulation vector	$\mathbf{q}_p = 0.9208(6)\mathbf{c}^*$	—
Refinement method	Program Jana2006	Program Jana2006
x_{O1}	0.223 52(22)	0.222 87(14)
y_{O1}	0.273 10(22)	0.273 80(14)
y_{O1}	0.080 61(20)	0.080 73(13)
x_{O2}	0.342 33(19)	0.342 39(12)
y_{O2}	0.521 94(16)	0.522 07(11)
y_{O2}	0.341 12(36)	0.341 25(24)
R_p	5.53	3.49
R_{wp}	7.69	4.88

with increasing intensities upon cooling. The Miller indices of the satellites $(h, k, l+q_p)$ or $(h, k, l-q_p)$ are shown in figure 2. At least 16 satellite Bragg reflections have been observed in neutron powder diffraction patterns below 290 K.

The Rietveld refinements shown in figure 2 have been carried out with the model of atomic position modulations derived from our $CaMn_7O_{12}$ SR diffraction studies [13]. The length of the propagation vector q_p was refined but the amplitudes of the atomic position modulations were assumed to be the same as those in table 2 in [13]. The refined value of $q_p = 0.9231(12)c^*$ for $CaMn_7O_{12}$ at 10 K is close to that obtained from the earlier synchrotron x-ray diffraction results $q_p = 0.9203(1)c^*$ [13]. The quality of the neutron powder diffraction refinement shown in figure 2 is excellent and our attempts to refine the modulation amplitudes did not lead to improved fits.

The modulation of the atomic positions in $CaMn_7O_{12}$ can be either described using the 'long' modulation vector $q_p \approx 0.92$, as discussed in [13], or a 'short' modulation vector $q'_p = (1-q_p) \approx 0.08$, as proposed in [16]. A quantitative description of the modulated structure with the 'short' propagation vector requires an additional centering in the fourth dimension [23]. In the present paper we use the 'long' propagation vector due to its simplicity [13]. Figure 3 shows the modulation of the z coordinate of the Mn ions in the Mn3 sublattice (Wyckoff site (3b) in space group $R\bar{3}$) as a function of the position along the c-axis. The descriptions with the 'long' modulation vector (solid line) and with the 'short' modulation vector (dashed line) give the same atomic positions, as shown in figure 3. In the following sections we will analyze the modulation length, L_p, that corresponds to the 'short' propagation vector, i.e.

$$L_p = \frac{2\pi}{c^*}\frac{1}{(1-q_p)}.$$

The modulation length, L_p, is close to 81.2(1) Å as shown in figure 3.

The new powder neutron diffractograms are particularly important for an unambiguous determination of the atomic modulations in $CaMn_7O_{12}$. Previous powder neutron diffraction experiments only covered a limited Q-range with no obvious satellite peaks [16] in the measured region. The currently accepted description of the modulated structure of

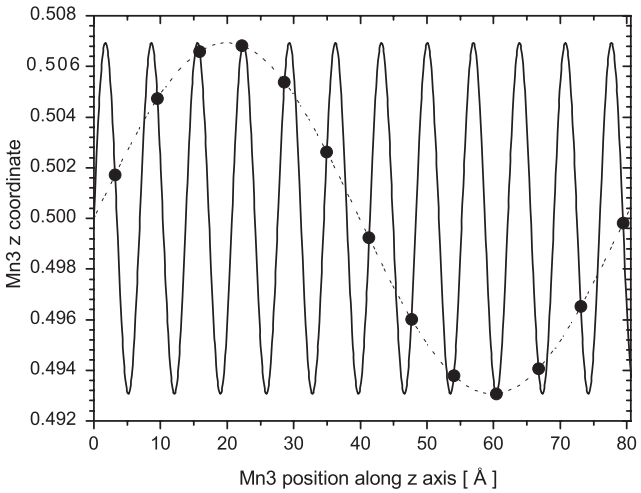

Figure 3. Modulation of the z-coordinate of the Mn3 sublattice in $CaMn_7O_{12}$ at 10 K [13]. Solid points = Mn3 positions located at (0 0 0.5) in subsequent unit cells; solid line = modulation corresponding to the 'long' modulation vector $q_p = 0.9224(13)c^*$; dashed line = modulation corresponding to the 'short' $(1 - q_p)$ modulation vector.

$CaMn_7O_{12}$ was derived from synchrotron based powder x-ray diffractograms [13] and permitted the simulation of powder neutron diffractograms. Only very weak neutron diffraction satellite peaks (below the signal to noise ratio) were predicted for the previously measured neutron data and thus the neutron data did not contradict the model [13, 16] but still left some doubts regarding its correctness.

However, the latest neutron diffraction data provide sufficient counting statistics and cover a large enough Q-range for the measurement of a sufficiently large number of neutron diffraction satellite peaks, and therefore permitted us to unambiguously determine the modulated structure of $CaMn_7O_{12}$. This structure is in agreement with the previously reported modulated structure [13].

In conclusion the present neutron diffraction study of $CaMn_7O_{12}$ carried out with diffractometer D2B independently confirms the quantitative model of the modulation of atomic positions, Mn–O distances and Mn–O–Mn angles that are shown in figures 4–7 in [13].

3.2. Magnetic modulation

The neutron diffraction measurements show the onset of magnetic long range ordering with Néel temperatures, T_N, equal to 90.4, 89.2 and 78.1 K for $CaCu_xMn_{7-x}O_{12}$ where $x = 0.0$, 0.1 and 0.23, respectively [13].

Previously the low temperature magnetic structure of $CaMn_7O_{12}$ was described as two coexisting magnetic phases: (1) a ferrimagnetic phase and (2) a modulated magnetic phase [7, 10]. Furthermore it was reported that at 50 K the ferrimagnetic phase undergoes a phase transition to another modulated magnetic structure with a strong magnetic modulation dependence as a function of temperature. Therefore below 50 K the presence of two coexisting modulated magnetic structures was assumed [7, 10, 24].

In contrast our present neutron powder diffraction study shows that all the magnetic Bragg peaks can be described with a single modulated magnetic phase with magnetic modulation vector $\vec{q}_m$ parallel to the c-axis. Figure 4 shows the low-angle parts of the neutron powder diffractograms of $CaMn_7O_{12}$ (new CMO_B sample) measured on diffractometer D2B at 10, 60, 100 and 290 K. Note that all satellite peaks are magnetic peaks because no structural satellite peaks are observable in this angular range. The refinements were carried out in the pattern-matching mode where the magnetic peaks are described as $(h, k, l \pm q_m)$ Bragg peaks. During the refinement in the pattern-matching mode the intensities of the magnetic peaks are fitted independently, consequently the modulation

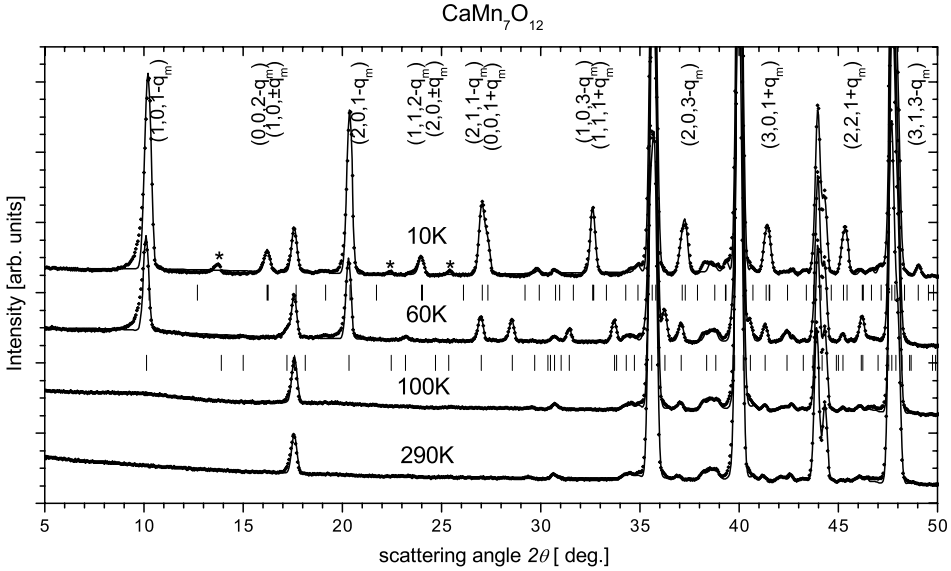

Figure 4. Selected parts of the neutron powder diffraction patterns of $CaMn_7O_{12}$ (sample CMO_B) measured at 10, 60, 100 and 290 K. Solid symbols indicate measured data while the solid line represents the calculated profile obtained in pattern matching. The indexing of the magnetic Bragg peaks is shown above the diffraction pattern. Stars indicate three maxima that could not be indexed.

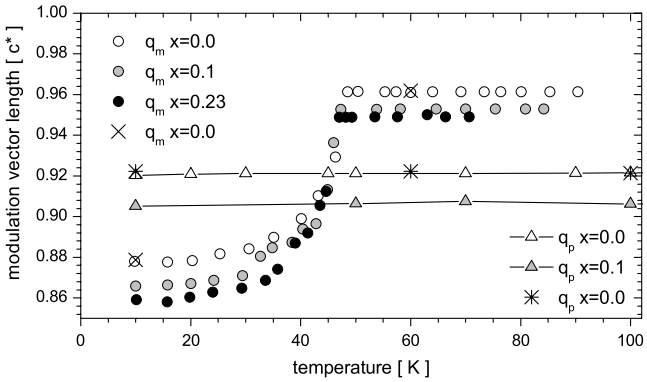

Figure 5. Temperature dependence of the magnetic modulation vector length q_m for $CaCu_xMn_{7-x}O_{12}$ ($x = 0.0$ (open circles), 0.1 (gray circles) and 0.23 (black circles)) (samples CMO_A, CC1MO_A and CC2MO_A) measured on neutron diffractometer D20. Two additional points show q_m values obtained on neutron diffractometer D2B for $CaMn_7O_{12}$ (crosses) (sample CMO_B). The temperature dependence of atomic position modulation vector q_p for $CaCu_xMn_{7-x}O_{12}$ ($x = 0.0$ (open triangles) and 0.1 (gray triangles)) measured by synchrotron radiation diffractometer ID31 and for $x = 0.0$ (asterisk) measured with neutron diffractometer D2B.

vector q_m can be obtained but the magnitudes of the magnetic moments cannot be determined. At $T = 60$ K all the magnetic Bragg peaks for $CaCu_xMn_{7-x}O_{12}$ are successfully described with a single propagation vector. At 10 K all but three weak Bragg peaks (marked with (*) in figure 4) are indexed. The present analysis of one low temperature modulated magnetic phase gives a more coherent model than the complex two phase magnetic model reported earlier [7].

In an effort to follow the magnetic structure evolution in detail powder neutron diffraction experiments were carried out on the high-flux neutron diffractometer D20 collecting data sets in approximately 5 K increments from 10 to 80 K. Figure 5 compares the temperature evolution of the length of the magnetic modulation vector, q_m, with the structural, q_p, propagation vector for $CaCu_xMn_{7-x}O_{12}$ ($x = 0.0$, 0.1 and 0.23)

Near 50 K a magnetic phase transition with a significant change of the magnetic modulation vector length q_m is observed for all $CaCu_xMn_{7-x}O_{12}$ samples, whereas the atomic modulation vector q_p is almost constant between 10 and 100 K. There is a satisfactory agreement between results obtained for different $CaMn_7O_{12}$ samples measured with different instruments. One can compare results for undoped $CaMn_7O_{12}$: the new CMO_B sample measured with neutrons on D2B (both q_m and q_p) and the older CMO_A sample measured with neutrons on D20 (q_m) and with SR on ID-31(q_p).

Similar steep changes of q_m below the transition temperature of 50 K are observed for all $CaCu_xMn_{7-x}O_{12}$ ($x = 0.0$, 0.1 and 0.23). Recent studies with $CaMn_7O_{12}$ have shown a considerable enhancement of the magnetoelectric coupling below the magnetic transition temperature of 50 K [8]. It is therefore possible that the $x = 0.1$ and 0.23 doped compounds will also show an enhancement of the magnetoelectric coupling below 50 K.

3.3. Comparison of the modulation of the atomic positions and magnetic moments

The values of both propagation vectors q_m and q_p are almost constant in the temperature range between the magnetic phase transition at 50 K and the Néel temperature. Their values show the following relation:

$$(1 - q_p) = 2(1 - q_m)$$

i.e. the length of the modulation of atomic positions L_p is half the length of the modulation of the magnetic moments L_m. Figure 6 shows the relation by comparing values of $(1 - q_p)$ and $2(1 - q_m)$ for the 50 K $< T <$ T_N. The error bars indicate the spread of $(1-q_p)$ and $2(1-q_m)$ values over the temperature range 50 K $< T <$ T_N. For the sake of clarity the results for different experiments and samples have been plotted on two separate graphs.

Figure 6(a) shows data obtained for CMO_A, CC1MO_A and CC2MO_A with SR powder diffraction (ID31 ESRF) and neutron powder diffraction studies (D20 ILL). Figure 6(b) presents data obtained for the CMO_B sample in the present neutron powder diffraction study (D2B ILL). The relation $L_m = 2L_p$ is expected for a model system with spin density

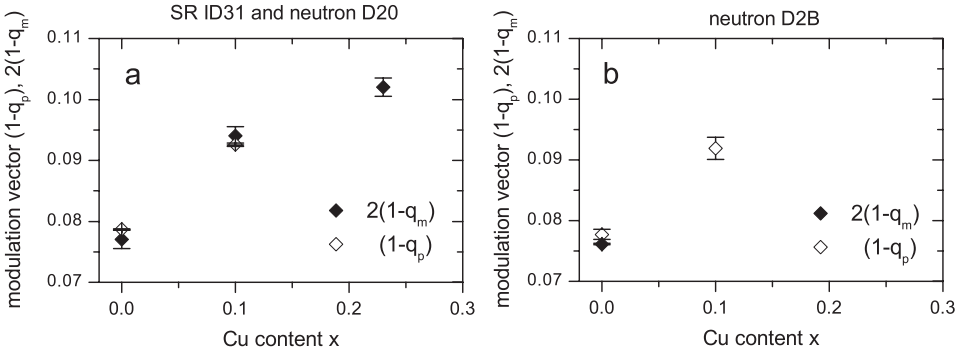

Figure 6. Comparison of the length of the modulation of atomic positions and modulation of the magnetic moments for $CaCu_xMn_{7-x}O_{12}$ ($x = 0.0$, 0.1 and 0.23) describing the temperature range 50 K $< T <$ T_N. The vertical axis presents the value the of 'short' atomic position modulation vector $(1 - q_p)$ and the magnetic modulation vector $2(1 - q_m)$ as a function of the Cu concentration x in $CaCu_xMn_{7-x}O_{12}$. Panel (a) shows results obtained from SR ID31 and neutron D20 data for $CaCu_xMn_{7-x}O_{12}$ where $x = 0.0$, 0.1 and 0.23 (CMO_A, CC1MO_A and CC2MO_A) as reported in [13, 16] and panel (b) illustrates results obtained from neutron data D2B (present studies). Note that no modulation of atomic positions has been observed in $CaCu_{0.23}Mn_{6.8}O_{12}$ (panel (a)).

wave magnetic modulation and magnetoelastic coupling where the exchange integral depends linearly on the interatomic distance [25]. This relation of the magnetic and positional modulation lengths $L_m = 2L_p$ has been observed in numerous materials including chromium [26, 27], thulium [28], $Ce(Ru_{1-x}Rh_x)Si_2$ [29] and $CuFe_{1-x}Al_xO_2$ [30]. The magnetic ordering in $CaCu_xMn_{7-x}O_{12}$ has not been completely solved, consequently it is not yet possible to propose a quantitative model of the magnetoelastic interactions.

We conclude with the following major findings. The previously reported modulation of the atomic positions observed with SR powder diffraction [13] in $CaCu_xMn_{7-x}O_{12}$ ($x = 0.0$ and 0.1) has now been confirmed independently with neutron diffraction measurements. The relation of positional and magnetic modulation lengths $L_m = 2L_p$ between 50 K and the Néel temperature for $CaCu_xMn_{7-x}O_{12}$ suggests magnetoelastic coupling. The magnetic transition for $CaCu_xMn_{7-x}O_{12}$ at 50 K is the result of the change of the magnetic modulation length. Consequently the magnetic structure of $CaCu_xMn_{7-x}O_{12}$ is now characterized with a single phase magnetic model. The magnetic phase transition observed in $CaMn_7O_{12}$ [7] near 50 K has now also been observed for Cu doped $CaCu_xMn_{7-x}O_{12}$ ($x = 0.1$ and 0.23) members. It is therefore likely that these $CaCu_xMn_{7-x}O_{12}$ compounds also show magnetoelectric coupling. Further studies of these compounds are in progress.

Acknowledgments

Thanks are due to E Suard for assistance and help with the neutron diffraction measurements at the ILL in Grenoble. Thanks are due to the ILL and ESRF for beamtime. Thanks are due to the Ministry of Science and Higher Education (Poland). MB acknowledges the financial support from the Natural Sciences and Engineering Research Council (NSERC) of Canada, the Canada Foundation for Innovation (CFI) and the Manitoba Research Innovation Fund.

References

[1] Fiebig M 2005 *J. Phys. D: Appl. Phys.* **38** R123
[2] Ederer C and Spaldin N A 2005 *Curr. Opin. Solid State Mater. Sci.* **9** 128
[3] Katsura H, Nagaosa N and Balatsky A V 2005 *Phys. Rev. Lett.* **95** 057205
[4] Mostovoy M 2006 *Phys. Rev. Lett.* **96** 067601
[5] Kimura T, Sekio Y, Nakamura H, Siegrist T and Ramirez A P 2008 *Nat. Mater.* **7** 291
[6] Ishiwata S, Taguchi Y, Murakawa H, Onose Y and Tokura Y 2008 *Science* **319** 1643
[7] Przeniosło R, Sosnowska I, Hohlwein D, Hauss T and Troyanchuk I O 1999 *Solid State Commun.* **111** 687
[8] Sánchez-Andújar M, Yáñez-Vilar S, Biskup N, Castro-García S, Mira J, Rivas J and Señaris-Rodríguez M 2009 *J. Magn. Magn. Mater.* **321** 1739
[9] Vasil'ev A N and Volkova O S 2007 *Low Temp. Phys.* **33** 895
[10] Przeniosło R, Sosnowska I, Żółtek M, Hohlwein D and Troyanchuk I O 1998 *Physica* B **241–243** 730
[11] Castro-Couceiro A, Yáñez-Vilar S, Sánchez-Andújar M, Rivas-Murias B, Rivas J and Señaris-Rodríguez M A 2007 *Prog. Solid State Chem.* **35** 379
[12] Yáñez-Vilar S, Castro-Couceiro A, Rivas-Murias B, Fondado A, Mira J, Rivas J and Señaris-Rodríguez M A 2005 *Z. Anorg. Alleg. Chem.* **631** 2265
[13] Sławiński W, Przeniosło R, Sosnowska I, Bieringer M, Margiolaki I and Suard E 2009 *Acta Crystallogr.* B **65** 535
[14] Sears V 1992 *Neutron News* **3** 26
[15] Sławiński W, Przeniosło R, Sosnowska I, Bieringer M, Margiolaki I, Fitch A N and Suard E 2006 *J. Solid State Chem.* **179** 2443
[16] Sławiński W, Przeniosło R, Sosnowska I, Bieringer M, Margiolaki I, Fitch A N and Suard E 2008 *J. Phys.: Condens. Matter* **20** 104239
[17] Hadermann J, Abakumov A M, Gillie L J, Martin C and Hervieu M 2006 *Chem. Mater.* **18** 5530
[18] Barrier N, Michel C, Maignan A, Hervieu M and Raveau B 2005 *J. Mater. Chem.* **15** 386
[19] Rietveld H 1969 *J. Appl. Crystallogr.* **2** 65
[20] Petricek V, Dusek M and Palatinus L 2006 *The Crystallographic Computing System* (Praha, Czech Republic: Institute of Physics)
[21] Bochu B and Buevoz J L 1980 *Solid State Commun.* **36** 133
[22] Przeniosło R, Sosnowska I, Suard E, Hewat A and Fitch A N 2004 *Physica* B **344** 358
[23] Van Smaalen S 2009 *Incommensurate Crystallography* (New York: Oxford Science Publications)
[24] Przeniosło R, Sosnowska I, Strunz P, Hohlwein D, Hauss T and Troyanchuk I 2000 *Physica* B **276–278** 547
[25] Lovesey S W and Collins S P 1996 *X-Ray Scattering and Absorption by Magnetic Materials* (Oxford: Clarendon) chapter 2.1.3 (Magnetically Induced Charge Scattering) p 51
[26] Tsunoda Y, Nakai Y and Kunitomi N 1975 *Solid State Commun.* **16** 443
[27] Fawcett E 1988 *Rev. Mod. Phys.* **60** 209
[28] Bohr J, Gibbs D and Huang K 1990 *Phys. Rev.* B **42** 4322
[29] Tabata Y, Okita Y, Kanadani C, Taniguchi T, Kawarazaki S and Uwatoko Y 2005 *Physica* B **359–361** 263
[30] Nakajima T, Mitsuda S, Inami T, Terada N, Ohsumi H, Prokes K and Podlesnyak A 2008 *Phys. Rev.* B **78** 024106